Food Hydrocolloids 142 (2023) 108864

Contents lists available at ScienceDirect

Food Hydrocolloids

journal homepage: www.elsevier.com/locate/foodhyd

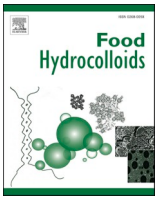

Carvacrol/cyclodextrin inclusion complex loaded gelatin/pullulan nanofibers for active food packaging applications

Kubra Ertan [a,c,d], Asli Celebioglu [a], Rimi Chowdhury [b], Gulum Sumnu [c], Serpil Sahin [c], Craig Altier [b], Tamer Uyar [a,*]

[a] Fiber Science Program, Department of Human Centered Design, College of Human Ecology, Cornell University, Ithaca, NY, 14853, United States
[b] Department of Population Medicine and Diagnostic Sciences, College of Veterinary Medicine, Cornell University, Ithaca, NY, 14850, United States
[c] Department of Food Engineering, Middle East Technical University, 06800, Ankara, Turkey
[d] Department of Food Engineering, Faculty of Engineering and Architecture, Burdur Mehmet Akif Ersoy University, Istiklal Campus, 15030, Burdur, Turkey

ARTICLE INFO

Keywords:
Carvacrol
Cyclodextrin
Electrospinning
Antibacterial and antioxidant
Fish oil oxidation
Active food packaging

ABSTRACT

Carvacrol is a natural essential oil with a monoterpenoid structure and draws attention due to its antimicrobial and antioxidant capacity. However, high volatility and hydrophobicity limit its use in food packaging systems. This hindrance can be overcome by the complexation with cyclodextrins. In this study, the inclusion complexes (IC) of gamma-cyclodextrin (γCD) and carvacrol were integrated into gelatin/pullulan nanofibers. The control sample of carvacrol loaded gelatin/pullulan nanofibers were generated, as well. Both nanofibers indicated a free-standing and flexible character with defect-free morphology. The carvacrol-γCD-IC crystals were obviously detected within the gelatin/pullulan nanofiber structure differently from carvacrol loaded one. The inclusion complexation of γCD with carvacrol decreased the loss of this essential oil during electrospinning significantly ($p < 0.05$). Carvacrol retention was determined as 67.84% and 57.63% after two months of storage at room temperature for the carvacrol-γCD-IC and carvacrol loaded gelatin/pullulan nanofibers, respectively. Here, inclusion complexation played a key role in enhancing thermal stability and antibacterial performance of carvacrol loaded in the gelatin/pullulan nanofibers. The promising antioxidant property of nanofibers was revealed in food packaging applications by the accelerated shelf-life test at 40 °C. Oxidation of fish oil samples was retarded by carvacrol-γCD-IC loaded nanofibers. This study provided an understanding of the potential of carvacrol in active food packaging and how the inclusion complex with CD affected the physicochemical properties of this bioactive compound.

1. Introduction

Electrospinning technology is one of the promising approaches to produce food packaging materials (Aytac, Ipek, et al., 2017; Aytac, Keskin, et al., 2017; Yilmaz et al., 2022). This efficient, cost-effective, and versatile technique enables the production of antimicrobial and antioxidant nanofibers (Topuz & Uyar, 2020). Besides the porous structure and high surface area, electrospun nanofibers can encapsulate bioactive substances with high loading capacity and with release profile from fast to controlled/sustained (Weiss et al., 2012; Wen et al., 2017). Polysaccharides including starch (Fonseca et al., 2019), chitosan (Lin et al., 2018), alginate (Dai et al., 2022), pullulan (Celebioglu & Uyar, 2021) and proteins such as gelatin (Tang et al., 2019), whey (Sullivan et al., 2014), zein (Zhan et al., 2020) and soy protein (Kutzli et al., 2019) are biopolymers that have been used in formulations of electrospun packaging materials. However, additional chemical modification or carrier polymeric matrix can be required to remove the challenges from their branched and complex chemical structures of these biopolymers (Dierings de Souza et al., 2021).

In this study, pullulan and gelatin were combined to produce food-grade nanofibers. Gelatin, an animal-sourced protein, is widely used in the food industry as a stabilizing, emulsifying, thickening, and gelling agent for several food products. Additionally, it plays an essential role in developing edible coating and packaging (Hattrem et al., 2015; Karim & Bhat, 2008). Nowadays, fish gelatin has pronounced attention due to keeping away from religious concerns and apprehension about bovine spongiform encephalopathy (mad cow disease) while the primary commercial gelatin source is porcine skin (Nurilmala et al., 2022).

* Corresponding author.
E-mail address: tu46@cornell.edu (T. Uyar).

https://doi.org/10.1016/j.foodhyd.2023.108864
Received 11 February 2023; Received in revised form 18 April 2023; Accepted 8 May 2023
Available online 9 May 2023

Pullulan, synthesized by the yeast-like fungus *Aureobasidium pullulans,* is a linear polysaccharide consisting of maltotriose units. These units are formed by three glucose linked via α-1,4 glycosidic bonds, and between the maltotriose units α-1,6 glycosidic linkages are found (Trinetta & Cutter, 2016). This particular pattern of linkage and adhesive properties provide distinct characteristics to pullulan including the ability to produce fibers and oxygen-impermeable, robust coatings (Kraśniewska et al., 2019). On the other hand, pullulan is hydrophilic due to hydrogen bonding capacity. Pullulan electrospun nanofibers have previously been used in antibacterial food packaging systems with the bioactive ingredients such as nisin (Soto et al., 2019), polyphenols (Shao et al., 2018) and resveratrol (Seethu et al., 2020).

Carvacrol, found in oregano and thyme essential oils, is a phenolic monoterpene compound having the chemical structure of 5-isopropyl-2-methyl phenol. The phenolic OH group and substituted aromatic ring of carvacrol have resulted in strong antioxidant properties and hydrophobicity (Friedman, 2014). Moreover, carvacrol demonstrates inhibitory effect against a wide range of microorganisms, including food-borne pathogens (Bayir et al., 2019). Carvacrol-incorporated nanofibers have been previously applied to extend the shelf-life of wheat bread (Altan et al., 2018), pork (Guo et al., 2020) and strawberry (Wong et al., 2022). In this study, carvacrol-loaded nanofibers were applied as food packaging material to prevent fish oil oxidation. Because the long-chain ω-3 fatty acids in fish oil easily decompose to hydroperoxides and secondary oxidation products responsible for off-flavors. Oxidation susceptibility restricts the use of fish oil as a food ingredient and dietary supplement (Miyashita et al., 2018).

Cyclodextrins (CDs), the cyclic oligosaccharides, are starch-derived molecules with α-1,4-linked glucose units in truncated conic shape. The external wall has a hydrophilic character due to hydroxyl groups, while the inner surface shows a hydrophobic nature attributed to glycosidic bond orientations Therefore, the inner cavity enables the non-covalent inclusion complexation with hydrophobic compounds (Cid-Samamed et al., 2022; Crini et al., 2018; Y. Liu et al., 2022). Inclusion complexation with volatile compounds acquires the enhancement in thermal and oxidative stability, efficient encapsulation, and controlled release of active compound without hindering from bioactivity (Cid-Samamed et al., 2022; Hadian et al., 2023; Y. Liu et al., 2022). In this study, γCD was used to form inclusion complexes (IC) with carvacrol molecules (Fig. 1).

In the present study, pullulan, an edible polymer with a non-toxic, odorless, and tasteless character, was chosen as the polysaccharide because of its remarkable electrospinnability features, ability to create nanofibers, and form hydrogen bonding with proteins (Gounga et al., 2007; Trinetta & Cutter, 2016). Gelatin was selected as the protein part which is compatible with pullulan, and could produce versatile electrospun nanofibers. There have been studies conducted on producing electrospun nanofiber with the incorporation of gelatin and pullulan to create food packaging material (Shen et al., 2022; Wang et al., 2019, 2021). Even, the physicochemical properties of gelatin-pullulan-based nanofibers has been investigated in these reports (Wang et al., 2019), in which crosslinking (Wang et al., 2021) or modification by glycation (Shen et al., 2022) were performed. However, none of them have assessed the potential of this nanofiber system as a food packaging material with an actual food application test. Additionally, there is no study in the literature in which gelatin-pullulan nanofibers were incorporated with the essential oils or with their cyclodextrin inclusion complexes to enhance the stability of these active compounds and to exhibit their effect on the characteristic properties of the gelatin-pullulan-based nanofibers. In this study, carvacrol-γCD-IC were early incorporated in the gelatin-pullulan nanofibers for the purpose of active food packaging. The structural examination and the potential of these nanofibers as active food packaging were evaluated using proper techniques and antioxidant, antimicrobial, peroxide value, and conjugated diene measurement. Carvacrol-loaded gelatin/pullulan nanofibers were also generated for the comparative analysis.

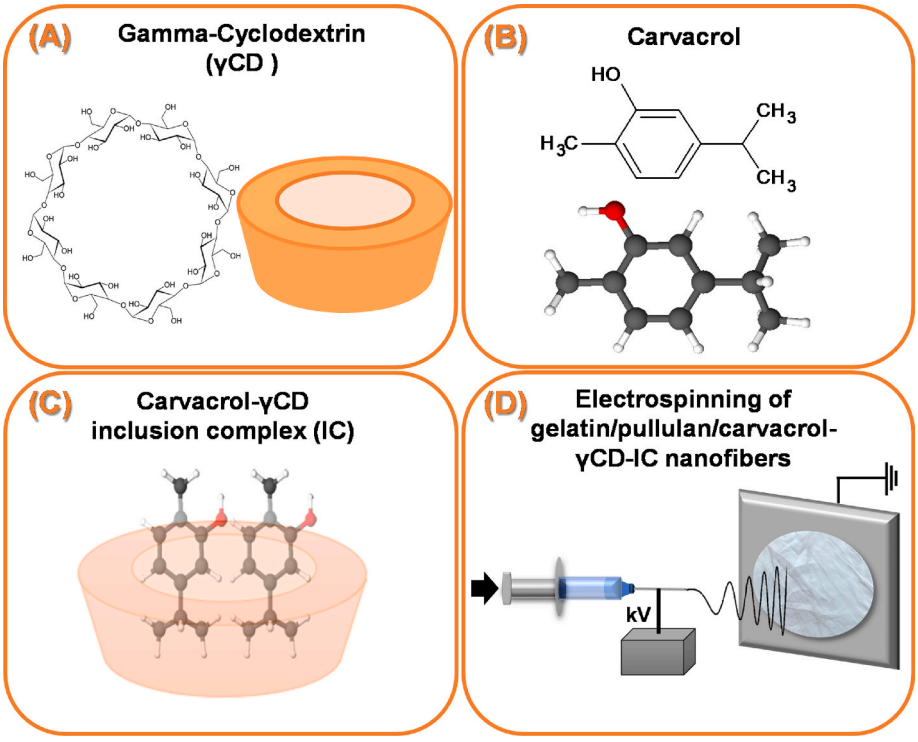

Fig. 1. The chemical structure of (A) γCD and (B) carvacrol. (C)The schematic representation of inclusion complex formation between γCD and carvacrol. (D) The schematic representation of the electrospinning of gelatin/pullulan/carvacrol-γCD-IC nanofibers.

2. Materials and methods

2.1. Materials

Carvacrol (CRV) (98%, Sigma-Aldrich), gelatin from cold water fish skin (Sigma-Aldrich), pullulan (Mw: 300 000 g/mol, TCI America), dimethyl sulfoxide (DMSO, >99.9%, Sigma-Aldrich), methanol (≥99.8%, Sigma-Aldrich), 2,2-diphenyl-1-picrylhydrazyl (DPPH, ≥97%, TCI America), fish oil (Spectrum Chemical MFG Corp), chloroform (99–99.4%, Merck), isooctane (2,2,4-Trimethylpentane, Aqua Solutions), sodium thiosulfate (Fisher Chemical) and potassium iodide (99%, Thermo Scientific) were provided commercially. Gamma cyclodextrin (γCD, Cavamax W8 Food) was supplied from Wacker Chemie AG (USA) as a kind gift. Millipore Milli-Q ultrapure water system (Millipore, USA) was used to distill the water.

2.2. Methods

2.2.1. Preparation of carvacrol-γCD-inclusion complexes and electrospinning systems

The inclusion complexes (IC) of carvacrol and γCD were prepared by adding carvacrol at molar ratio of 1:2 (γCD:carvacrol). Firstly, the γCD was dissolved at the concentration of 16% (w/v) in water by continuous stirring at room temperature. When the clear solution was obtained, carvacrol was added to the aqueous γCD solution for forming inclusion complexes (IC). Here, γCD was chosen instead of the other two native CD types (αCD and βCD) due to its higher water solubility (232 g/L) compared to others (145 g/L and 18.5 g/L) (Valle & Del, 2004). This enabled to dissolution higher amount of CD in the aqueous medium of electrospinning solution and so to attain the inclusion complex system having a higher ratio within the ultimate nanofibrous sample. Additionally, γCD has a bigger cavity size compared to αCD and βCD and this also allowed preparation inclusion complexes with a 1:2 (host:guest) molar ratio (Aytac, Ipek, et al., 2017). The IC solution was stirred overnight at room temperature and white aqueous system was obtained confirming the formation of IC crystals. Afterwards, pullulan (9%, (w/v)) was added to the IC solution and continued to be stirred. Then, glacial acetic acid was added to the solution so as to provide acetic acid/water 3/7 (v/v) ratio and to dissolve the second polymer gelatin (9%, w/v) at room temperature. The carvacrol content of gelatin/pullulan/carvacrol-γCD-IC (GEL/PUL/CRV-γCD-IC NF) nanofibers was 10% (w/w), so the solution of the control sample of gelatin/pullulan/carvacrol nanofibers (GEL/PUL/CRV NF) was prepared to have the same carvacrol content (10%, w/w). The three different electrospinning solutions (GEL/PUL, GEL/PUL/CRV, and GEL/PUL/CRV-γCD-IC) were individually loaded to 1 mL syringe having the metallic needle (27 G) and delivered to the system using a horizontal syringe pump. The grounded rectangular metal collector (15 × 15 cm) was covered by aluminium foil and placed across the needle in electrospinning equipment (Spingenix, model: SG100, Palo Alto, USA). Optimized electrospinning parameters were constant flow rate at 1.0 mL/h, high voltage at 13 kV, and 15 cm distance between the needle tip and metal collector. Electrospinning was performed under the ambient conditions of 23% relative humidity and 20 °C. The solution parameters such as viscosity and conductivity for each solution were determined using appropriate equipment preceding electrospinning. Conductivity was measured by a conductivity meter (FiveEasy, Mettler Toledo, USA) at room temperature. The apparent viscosity of solutions at 20 °C was measured by a rheometer (AR 2000 rheometer, TA Instrument, USA) equipped with 4° cone-plate (20 mm) spindle at a shear rate of 0.01–1000 s^{-1}.

2.2.2. Scanning electron microscopy (SEM) characterization

The morphology of GEL/PUL NF, GEL/PUL/CRV NF, and GEL/PUL/CRV-γCD-IC NF was visualized by scanning electron microscope (SEM, Tescan MIRA3, Czech Republic). Before measurement, samples were coated with layer of Au/Pd to avoid charging issues. The SEM images of nanofibers were obtained at 12 kV accelerating voltage with distance of 10 mm and then processed by Image J software to calculate the average diameter of fibers taking into account randomly selected 100 nanofibers.

2.2.3. X-ray diffraction

The X-ray diffraction patterns of GEL/PUL NF, GEL/PUL/CRV NF, and GEL/PUL/CRV-γCD-IC NF were scanned over the 2Θ angles of 5° and 30° using X-ray diffractometer (XRD, Bruker D8 Advance ECO). Cu-Kα radiation was applied under the conditions of 40 kV and a current of 25 mA.

2.2.4. The Fourier transform infrared spectroscopy (FTIR)

The Fourier transform infrared spectra of gelatin, pullulan, γCD, carvacrol, GEL/PUL NF, GEL/PUL/CRV NF, and GEL/PUL/CRV-γCD-IC NF were obtained by the attenuated total reflectance Fourier transform infrared spectrometer (ATR-FTIR, PerkinElmer, USA). Measurements were carried out in the range of 4000–600 cm^{-1}. The spectra were collected at 4 cm^{-1}resolution by 64 scans.

2.2.5. Thermal characterization

The thermal profile of carvacrol, GEL/PUL NF, GEL/PUL/CRV NF, and GEL/PUL/CRV-γCD-IC NF was characterized by a thermogravimetric analyzer (TGA, Q500, TA Instruments, USA). The samples were weighed into a platinum pan, and analysis was performed in the range of 30°C–600 °C under the nitrogen atmosphere with a heating rate of 20 °C/min.

2.2.6. Encapsulation efficiency and shelf-life test

The predetermined amount of (~4 mg) GEL/PUL/CRV NF and GEL/PUL/CRV-γCD-IC NF were weighed and dissolved in 5 mL dimethyl sulfoxide (DMSO) separately. Three replicates were prepared for each sample. The DMSO solutions were stirred at room temperature for 30 min. The UV–Vis absorbance values of samples were measured at 278 nm by UV–Vis-spectrophotometer (PerkinElmer, Lambda 35, USA). A calibration curve ($R^2 \geq 0.99$) of carvacrol with various concentrations was prepared in DMSO to calculate the encapsulation efficiency of carvacrol. The encapsulation efficiency (%) of carvacrol was calculated using the following equation;

$$\text{Encapsulation efficiency } (\%) = (C_e / C_i) \times 100 \quad (1)$$

where C_e and C_i are the extracted carvacrol concentration and the initial carvacrol concentration, respectively. The preserved carvacrol amount in nanofibers was monitored for two months shelf-life test considering weekly intervals until the fourth week. Each sample was stored in Petri dishes at room temperature and opened to the atmosphere.

2.2.7. Antioxidant activity test

The antioxidant activity of GEL/PUL NF, GEL/PUL/CRV NF and GEL/PUL/CRV-γCD-IC NF was determined by a 2,2-diphenyl-1-picrylhydrazyl (DPPH•) assay. The DPPH• radical scavenging activity of samples was evaluated against both concentration-dependent and time-dependent manner. The stoke solution of DPPH• in methanol (75 μM) was prepared and diluted to an absorbance less than 1.0 at 517 nm to obtain working solution. For the time-dependent test, ~3 mg of sample was dissolved in 6 mL of distilled water and then 300 μL of this solution was mixed with 2700 μL DPPH• working solution. The absorbance values of solutions were recorded at 517 nm for 48 h (0.25, 0.5, 1, 2, 4, 6, 8, 12, 24, and 48 h). For the concentration-dependent test, aqueous solutions of samples were prepared at five different concentrations ranging from 125 μg/mL to 2000 μg/mL. An aliquot volume (2700 μL) of DPPH• working solution was added to 300 μL of the sample-containing solutions and then stirred. The samples were incubated for 24 h in the dark at room temperature. UV–Vis spectroscopy was used to assess the decrease of DPPH• absorption (517 nm). Each experiment was carried

out in triplicate. The DPPH• radical scavenging activity of GEL/PUL NF, GEL/PUL/CRV NF, and GEL/PUL/CRV-γCD-IC NF was calculated using the following equation;

$$\text{DPPH}\bullet\ \text{Inhibition}\ (\%) = \left[\left(A_{control} - A_{sample}\right) / A_{control}\right] \times 100 \quad (2)$$

where $A_{control}$ is the absorbance of the DPPH• working solution, and A_{sample} is the absorbance values of sample solutions. The 50% inhibition (IC50) concentrations which represent the minimum quantity of sample required to reduce DPPH• absorbance by 50% were calculated using the concentration-dependent graph.

2.2.8. Food application

Commercial fish oil was used to determine the antioxidative capability of nanofibers during accelerated storage at 40 °C. Fish oil (~13 g) was transferred into 50 mL glass bottles. Nanofibers were cut into 3.5 cm diameter circles (~40 mg) and placed on the surface under the plastic lid of bottles. Fish oil samples were closed with nanofibrous mat-covered lids. As a control, fish oil was closed using a nanofiber-free lid. The internal headspace of the fish oil included the ambient air. All samples were kept in dark at 40 °C and 100 rpm by an orbital shaker for 16 days. For the oxidative stability test, samples were taken on days 0, 4, 8, 12, and 16 for the peroxide and conjugated diene measurements. The peroxide values (PV) of the fish oil were determined according to Wang et al. (2011) with some modifications. The fish oil (~2 g) was weighed in an Erlenmeyer and 30 mL of chloroform:glacial acetic acid (3:2, v/v) solvent mixture was added. Subsequently, 1 mL saturated potassium iodide (KI) solution was added. The mixture was shaken for 30 s and then kept in the dark at room temperature for 5 min. After incubation, 75 mL distilled water and 0.5 mL starch indicator (0.05%) were added. The liberated iodine was titrated against the 0.01 M sodium thiosulfate ($Na_2S_2O_3$) until the blue colour disappeared. The PV was calculated as meq O_2/kg oil by the equation below;

$$\text{PV}\ (\text{meq}/\text{kg}) = (C \times (V - V_0) \times 12.69 \times 78.8) / m \quad (3)$$

where C is the concentration of sodium thiosulphate solution (mol/L); V and V_0 represent the volumes of titrant consumption by the samples and the blank, respectively (mL); and m is the fish oil mass (g).

Conjugated dienes, the early-stage products of fish oil oxidation, were evaluated using the UV–Vis spectrum of the oil samples (Ferreira et al., 2018). Fish oil samples (~0.02 g) were dissolved in 6 mL isooctane and then diluted with isooctane to read absorbance between 0.1 and 0.8. As a blank, pure isooctane was placed. The conjugated diene contents were determined by using absorbance values at 232 and calculated using the following equation;

$$\text{Conjugated Diene} = A_{232} / (C \times l) \quad (4)$$

where A_{232} is the absorbance value at the wavelength of 232 nm. C is the final concentration of the fish oil sample (g/100 mL), and l is the optical path length (cm) or the cuvette width which is 1 cm.

2.2.9. Antibacterial activity

First, the antibacterial performance of nanofibers was examined using the disk-diffusion assay. For this, *Escherichia coli*, *Salmonella enterica* serovar Typhimurium 14028s and *Staphylococcus aureus* were maintained in LB broth and LB agar. Single colonies of each LB agar plate were dissolved in 1X sterile PBS (pH = 7.4) and the turbidity of the solution was measured. All bacterial solutions were prepared to a McFarland standard of ~0.5. Sterile cotton swabs were saturated with bacterial solutions and streaked on LB agar plates. Nanofibers or filter papers of the same diameter were placed in triplicate on streaked LB agar plates. Streptomycin solution (50 mg/mL) was spotted on filter paper of similar diameter and used as a positive control. These were incubated at 37°C overnight. The region of clear zones surrounding the nanofibers or Streptomycin (Zone of exclusion) was photographed in the BioRad ChemiDoc gel acquisition system.

Growth curve assay was also applied for analysing the antibacterial profile of nanofibers. For this, the same bacterial strains were grown overnight in LB broth. From saturated overnight cultures, fresh starter cultures were grown until OD_{600} reached 1. Equal volume of culture was then centrifuged at 5000×*g* for 10 min. The supernatant was discarded, and pellets were resuspended in 1 mL of LB with 100 mM 3-(N-morpholino) propanesulfonic acid (MOPS) (pH = 6.8). Different concentrations of each nanofiber in DMSO were added to a mix of LB with 100 mM MOPS and 10 μL of the bacterial suspension. OD_{600} was recorded every 30 min for 20 h in Biotek Synergy H1 microplate reader. Data were plotted on Graphpad Prism. The inhibition rate (%) was calculated by the equation below using sample-free DMSO as a control;

$$\text{Inhibition rate}\ (\%) = \frac{OD600_t^S - OD600_{t_0}^S}{OD600_t^C - OD600_{t_0}^C} \times 100 \quad (5)$$

where $OD600_{t_0}^S$ is the initial OD600 value, and $OD600_t^S$ is the OD600 value of the samples at the 20th hour. $OD600_{t_0}^C$ and $OD600_t^C$ are the values of the DMSO measured at the beginning and after 20 h, respectively. As control, growth curve assay test was also performed for the different concentration of pure carvacrol.

2.2.10. Statistical analyses

Statistical analyses were conducted using analysis of variance (ANOVA) to determine whether there is a significant difference between the samples ($p \leq 0.05$). Minitab 16 Statistical Software (Minitab Inc., State College, PA, USA) was used for all these ANOVA analyses. Tukey comparison test was used to determine the significant difference between applications ($p \leq 0.05$). All the analyses were performed in triplicate.

3. Results and discussion

3.1. Morphological characterization of nanofibers

Aqueous electrospinning solutions formed solely by proteins are inadequate to produce nanofiber due to the lack of interchain associations or entanglements. In the literature, there are different approaches for producing nanofiber from native or denatured forms of proteins such as the use of organic or alcohol-based solvents or mixing with other spinnable polymers (Mendes et al., 2017). In this study, gelatin was blended with the carbohydrate-based polymer pullulan at ratio of 1/1 (w/w), and gelatin/pullulan nanofibers were produced successfully using acetic acid/water 3/7 (v/v) solvent system. The polymer ratio in this blend is one of the most important parameters that affects nanofiber morphology and size (Drosou et al., 2018). By using the same gelatin/pullulan (1/1) ratio, both carvacrol and carvacrol-γCD-inclusion complex loaded nanofibers were obtained with initial 10% (w/w) of carvacrol amount. This initial ratio (10% (w/w)) corresponds to the molar ratio of 1:2 (γCD:carvacrol) for inclusion complex based system. Due to the bigger cavity volume of γCD (427 $Å^3$) compared to other two native CD (αCD: 174 $Å^3$ and βCD: 262 $Å^3$) (Valle & Del, 2004), γCD was chosen to form inclusion complexes with 1:2 M ratio which enables to attain complexes with higher number of active compounds in the CD cavities. Even one of the related studies showed that thymol, another essential oil compound of oregano, formed inclusion complexes with γCD at both 1:1 and 1:2 M ratio, however 1:2 provided better complexation efficiency compared to 1:1 with higher loading of thymol, enhanced thermal stability, and retention due to better size match (Aytac, Ipek, et al., 2017).

The photos of electrospinning solutions and electrospun nanofibers and their scanning electron microscopy (SEM) images were shown in Fig. 2. The gelatin/pullulan solution was homogenous and transparent as seen in Fig. 2A. While a yellowish colour was observed after the

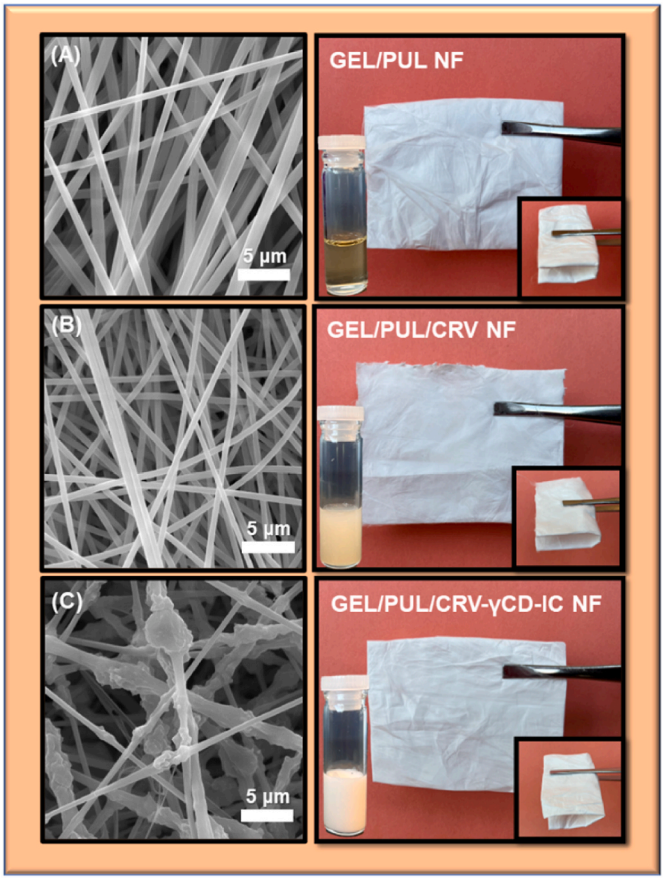

Fig. 2. The representative SEM images, the photos of electrospinning solutions, and the ultimate electrospun nanofibrous webs of (A) GEL/PUL, (B) GEL/PUL/CRV, and (C) GEL/PUL/CRV-γCD-IC NFs.

addition of carvacrol due to the emulsion like system formation (Fig. 2B), the crystals of carvacrol-γCD-inclusion complexes turned the colour of solution into white (Fig. 2C). The photo of carvacrol-γCD-inclusion complex solution taken just before the addition of polymers confirmed that the white colour of this system originated from the existence of inclusion complex crystals (Fig. S1). Here, it is noteworthy to mention that the precipitation or phase separation of polymers was not observed in the electrospinning solution which was used to generate nanofibers (Fig. 2A). Protein-polysaccharide interactions and their soluble complexes can be responsible for the stability of electrospinning solutions by the establishment of hydrogen bonds, hydrophobic interactions, and/or ionic bonds (Aceituno-Medina et al., 2013; Gounga et al., 2007). Here, both gelatin and pullulan were easily dissolved at a ratio of 9% (w/v) and this might have provided adequate interactions between these two polymers. As it has been previously reported, higher concentration of these polymers was also used to generate nanofiber by electrospinning. The continuous, pullulan-based nanofibers were obtained instead of a beaded structure when the amount of pullulan was raised from 10% to 20% in formic acid (95%) solution due to the increasing entanglements of polymer chains (Aceituno-Medina et al., 2013). Therefore, the acetic acid/water 3/7 (v/v) solvent system was not supposed to affect the pullulan, a non-ionic polysaccharide, spinnability or solution properties. It has been stated that the gelatin-based nanofiber was also fabricated by using solely 20% gelatin in acetic acid/water (3/1, v/v) (Mosayebi et al., 2022). Proteins are more dependent on pH than polysaccharides. As pH approaches the isoelectric point (pI), protein solubility decreases. However, the pH of the gelatin/pullulan solution was determined as 2.52 and this pH value was far from the fish gelatin (Type B) pI (pH 4.7–5.3) according to the type of gelatin used in this study. For all three systems, nanofibers were generated with free-standing and flexible features (Fig. 2). The uniform and homogenous nanofiber formation was observed for gelatin/pullulan nanofibers (GEL/PUL NF) and gelatin/pullulan/carvacrol nanofibers (GEL/PUL/CRV NF) (Fig. 2A and B). On the other hand, the SEM image of gelatin/pullulan/carvacrol-γCD-inclusion complex nanofibers (GEL/PUL/CRV-γCD-IC NF) indicated the distribution of inclusion complex crystals throughout the nanofibers (Fig. 2C). Inclusion complexes of γCD with eugenol in pullulan nanofibers demonstrated the similar crystal structures (Celebioglu & Uyar, 2021).

The solution properties and the average fiber diameter (AFD) values were summarized in Table 1. The AFD of GEL/PUL NF, GEL/PUL/CRV NF, and GEL/PUL/CRV-γCD-IC NF were determined as 520 ± 115 nm, 540 ± 85 nm, and 595 ± 205 nm, respectively. Morphology and size of nanofibers is significantly affected by the conductivity and viscosity of electrospinning solutions (Si et al., 2023; Zaitoon et al., 2021). Here, the addition of carvacrol into the electrospinning solutions did not drastically affect the solution conductivity or viscosity. Therefore, a notable difference was not observed between the AFD values of GEL/PUL NF and GEL/PUL/CRV NF. On the other hand, the inclusion complex included system caused distinct decrease at the conductivity value and an increase at the viscosity (Table 1). As expected, the incorporation of an additional solid substance; IC with the polymers in the electrospinning solution can result in more viscous system. On the other hand, gelatin is a polyelectrolytic polymer and shows higher conductivity than pullulan (Duconseille et al., 2015). Here, IC might have created a similar effect with pullulan due to the polysaccharide structure of γCD, and the dilution of the gelatin in the solution system might be responsible for the decreasing conductivity of GEL/PUL/CRV-γCD-IC solution (Drosou et al., 2018). Similar trends in conductivity and viscosity were also observed in polyvinyl alcohol (PVA) based electrospinning solutions which contained ICs of native CDs (α, β, and γCD) with vanillin (Kayaci & Uyar, 2012) and eugenol (Kayaci et al., 2013). Depending on lower conductivity and higher viscosity, less stretching was applied to the inclusion complex loaded system compared to other two during the electrospinning, and this led to thicker fiber formation (Si et al., 2023). The statistical analysis also displayed the significantly higher AFD value of GEL/PUL/CRV-γCD-IC NF compared to other two nanofibers with $p < 0.05$.

3.2. Structural characterization

The crystalline structure of samples was investigated using X-ray diffractometry (XRD). The XRD patterns of the GEL/PUL NF, GEL/PUL/CRV NF, and GEL/PUL/CRV-γCD-IC NF were presented in Fig. 3A. XRD was utilized to enquire about the inclusion complexation between CD and guest molecules in the sample (Narayanan et al., 2017). Here, both GEL/PUL NF and GEL/PUL/CRV NF had a similar broad halo in their diffractogram, indicating their amorphous structure. The addition of carvacrol didn't alter the crystalline structure of the GEL/PUL NF, and carvacrol molecule was distributed throughout the nanofibers without producing a crystal phase. Fundamentally, the crystalline pattern of inclusion complexation corresponds to the cylindrical channels by stacking CDs on top of each other and is called "channel-type" packing (Fig. S2B) whereas the pristine γCD possesses "cage-type" packing in which each CD cavity obstructs the neighbouring CD (Fig. S2A) (Celebioglu et al., 2017; Celebioglu & Uyar, 2021). Here, XRD graph of GEL/PUL/CRV-γCD-IC NF indicated the characteristic crystalline peaks at $2\theta = 7.5$, 14.2, 15.0, 15.9, 16.7, and 22.0° (Fig. 3A) presenting the channel-type packing that is quite different from the XRD pattern of pristine γCD having cage-type packing (Fig. S2C). This finding confirmed the formation and presence of the carvacrol-γCD-inclusion complex crystals within the GEL/PUL/CRV-γCD-IC NF (Celebioglu & Uyar, 2021).

Fourier transform infrared (FTIR) spectroscopy is one of the most widely used methods to determine the inclusion complex formation

Table 1
The solution properties and average fiber diameters (AFD) of nanofibers.

Sample	GEL (w/v)	PUL (w/v)	CRV (w/w)	γCD (w/v)	Viscosity (Pa.s)	Conductivity (μS/cm)	AFD (nm)
GEL/PUL NF	9	9	–	–	0.2239	1235	520 ± 115
GEL/PUL/CRV NF	9	9	10	–	0.2510	1233	540 ± 85
GEL/PUL/CRV-γCD-IC NF	9	9	10	16	0.5515	1034	595 ± 205

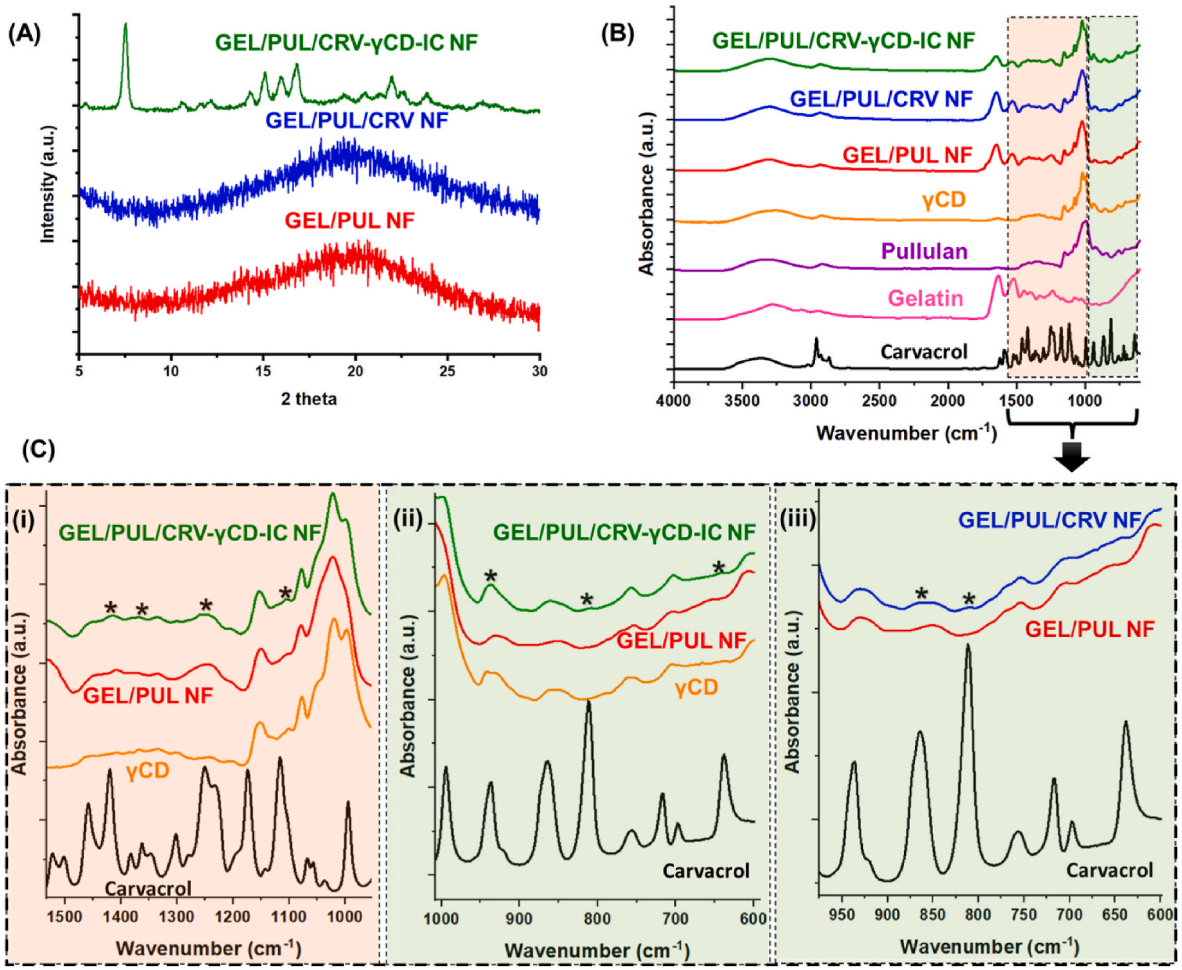

Fig. 3. (A) XRD patterns of GEL/PUL, GEL/PUL/CRV, and GEL/PUL/CRV-γCD-IC NFs. (B) The full range FTIR spectra of carvacrol, gelatin, pullulan, γCD, GEL/PUL NF, GEL/PUL/CRV NF, and GEL/PUL/CRV-γCD-IC NF. (C) The expanded range of FTIR spectra of carvacrol, γCD, GEL/PUL NF, and GEL/PUL/CRV-γCD-IC NF between (i) 1500-1000 cm^{-1}, (ii) 1000-600 cm^{-1} and (iii) the expanded range of FTIR spectra of carvacrol, GEL/PUL NF, and GEL/PUL/CRV NF between 980 and 600 cm^{-1}.

between cyclodextrin and guest molecules (Narayanan et al., 2017). Here, Fig. 3B showed the FTIR spectra and Fig. 3C indicated the expanded range FTIR spectra of samples. In the spectrum of carvacrol, the stretching peak of the –OH group was observed at 3368 cm^{-1} (Altan et al., 2018). The peak was around 2960 cm^{-1} associated with symmetric and asymmetric C–H stretching due to methyl groups (Valderrama & Rojas De, 2017). The distinctive absorption band originating from the aromatic ring of carvacrol between 1622 and 1420 cm^{-1} was specified as C–C stretching (Arrieta et al., 2013). The band at 1250 cm^{-1} is related to the C–O stretching of carvacrol. The key absorption bands of carvacrol were seen around 1116 and 994 cm^{-1} which were related to *ortho*-substitution and 1:2:4-substitution of carvacrol, respectively (Valderrama & Rojas De, 2017). The characteristic key band for carvacrol between 864 and 812 cm^{-1} is associated with the aromatic ring. The peak of out-of-plane C–H wagging vibrations, utilized to distinguish several types of aromatic ring substitutions, was located at about 812 cm^{-1} (Altan et al., 2018). In the FTIR spectra of γCD, a broad peak observed around 3268 cm^{-1} was associated with symmetrical and asymmetrical O–H stretching, while the peak around 2926 cm^{-1} was related to C–H stretching. The peak at 1642 cm^{-1} was represented as H–O–H bending of adsorbed water in γCD. Asymmetric stretching of C–O–C was detected at 1153 cm^{-1} and the bands at 1077 and 1020 cm^{-1} were attributed to C–O and C–C stretching (Celebioglu & Uyar, 2021; Kapoor et al., 2021).

FTIR spectrum of pullulan indicated a similar pattern with γCD due to α (1 → 4) linked glucopyranose units. Pullulan is a polymer that has maltotriose units made up of α (1 → 6) linked (1 → 4) α-d-triglucosides (Trinetta & Cutter, 2016). The spectrum of pullulan has characteristic peaks from O–H stretching (3330 cm^{-1}), C–H stretching (2918 cm^{-1}), H–O–H bending (1642 cm^{-1}), and C–O stretching (1200-1000 cm^{-1}). The characteristic peak of α-(1,6) glycosidic bonds, α-glucopyranosyl units, and α-(1,4) was presented at 930 cm^{-1}, 850 cm^{-1} and 754 cm^{-1}, respectively (Drosou et al., 2018; Islam & Yeum, 2013). The gelatin presented four identical absorption bands in the FTIR spectra at 3282

cm^{-1} (O–H stretching), 1634 cm^{-1} (C═O stretching), 1520 cm^{-1} (N–H bending with C–N stretching), and 1238 cm^{-1} (N–H stretching) that were associated with Amide A, Amide I, Amide II and Amide III, respectively (Ghorani et al., 2020). The other characteristic peak at 2934 cm^{-1} was Amide B corresponds to the asymmetric stretching vibration of = C–H and $-NH_3^+$ (Mosayebi et al., 2022). In our study, GEL/PUL NF absorption bands were located at the intensity between individual absorptions of gelatin and pullulan. The carvacrol presence in GEL/PUL/CRV NF was observed with the absorption bands at 864 and 812 cm^{-1} (Fig. 3C–iii). On the other hand, the absorption of bands at 938 cm^{-1}, 864 cm^{-1}, and 638 cm^{-1} indicated the presence of carvacrol in GEL/PUL/CRV-γCD-IC NF (Fig. 3C–ii). The expanded FTIR region indicating the absorption bands between 1500 and 1420 cm^{-1} (Fig. 3C–i) is related to the aromatic ring of carvacrol, and the shifts detected at the characteristic peaks of carvacrol proved the IC formation. Carvacrol interacts with the hydrophobic cavities of CD through its aromatic ring (Liu et al., 2021).

The thermal evaporation of volatile guest molecules can be retarded by forming inclusion complexes with cyclodextrin molecules (Mura, 2015). Therefore, the thermal stabilities and volatility of carvacrol and carvacrol loaded nanofibers were evaluated by thermogravimetric analysis (TGA). Fig. 4A indicates the relation between the mass-loss ratio of the samples and the temperature. The derivative thermogravimetric analysis (DTG) curve (Fig. 4B), which illustrates the weight loss rate as a function of temperature, showed that carvacrol underwent one-stage weight loss as a result of its evaporation at around 164 °C. The TGA thermograms of GEL/PUL NF exhibited three weight loss stages: the first stage was from 30 °C up to 100 °C, the second was at around 144 °C, and the last significant one was detected at 308 °C. The initial weight loss was attributed to water loss below 100 °C. The major weight loss at 308 °C and the small step at 144 °C corresponds to the degradation of gelatin/pullulan blend system. For GEL/PUL/CRV NF, there were also detected three main weight loss in the thermogram. Here, the moisture loss stage and the evaporation of carvacrol overlayed, and so a distinct step was observed at around 105 °C. The other small step (207 °C) and the big one (309 °C) was again due to the thermal degradation of the gelatin/pullulan blend. Meanwhile, GEL/PUL/CRV-γCD-IC NF did not display a noticeable weight loss step up to 200 °C except water loss (Fig. 4B). Here, the pattern that we had in case of GEL/PUL NF became sharper and more intense in shape with a step at 216 °C and at 319 °C due to the incorporation of CRV-γCD-IC crystals into nanofibers. This finding showed the encapsulated carvacrol in γCD cavities represented a delayed volatilization, so an enhanced thermal stability compared to its pristine state. It has been also reported in the previous studies involving various essential oils such as geraniol (P. P. Menezes et al., 2012), thymol (Tao et al., 2014), and eugenol (Celebioglu & Uyar, 2021).

3.3. Encapsulation efficiency and shelf-life of nanofibers

Carvacrol encapsulation efficiency after the electrospinning process and carvacrol preservation during two-months storage were evaluated for GEL/PUL/CRV NF and GEL/PUL/CRV-γCD-IC NF (Fig. 5). Both nanofibers were produced with the initial theoretical percentage of ~10% (w/w, mg carvacrol/mg NF) carvacrol. The encapsulation efficiency value for GEL/PUL/CRV NF right after the electrospinning was calculated as 70.58% ± 0.77, while the 90.62% ± 4.35 carvacrol retention was achieved for GEL/PUL/CRV-γCD-IC NF. The easy evaporation of the uncomplex carvacrol resulted in a higher loss in the GEL/PUL/CRV NF, and it was able to preserve carvacrol with 57.63% ± 1.30 at the end of the two months-storage. On the other hand, GEL/PUL/CRV-γCD-IC NF showed significantly higher preservation with 67.84% ± 0.61 after two months-storage ($p < 0.05$). The significant variations between the preservation values of these two samples were maintained during the whole storage period ($p < 0.05$). Here, the inclusion complexation ensured a better encapsulation profile for carvacrol in GEL/PUL/CRV-γCD-IC NF compared to GEL/PUL/CRV NF. A significant difference in the carvacrol preservation values was also observed during the fish oil storage test ($p < 0.05$). The preserved carvacrol values of GEL/PUL/CRV NF and GEL/PUL/CRV-γCD-IC NF used in the accelerated storage of fish oil as food packaging material were determined as approximately 64.70% and 88.68%, respectively. The findings proved that carvacrol stability was enhanced by inclusion complexation with γCD during the electrospinning process, storage at room temperature, and food packaging application at 40 °C.

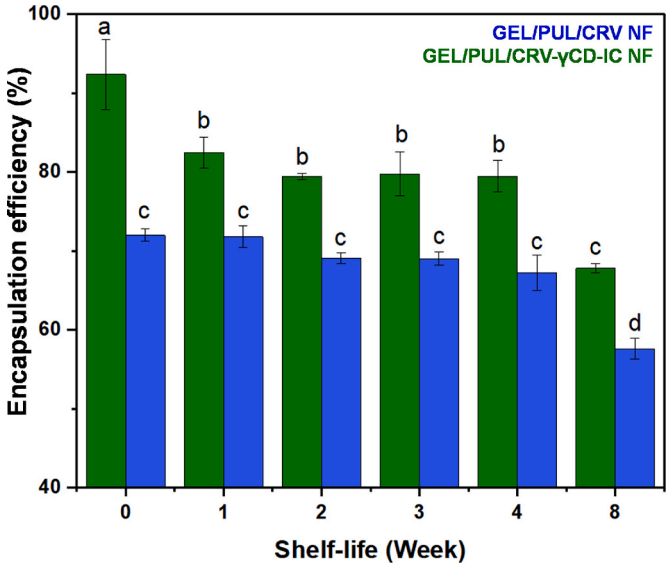

Fig. 5. Carvacrol encapsulation efficiency (%) of GEL/PUL/CRV NF and GEL/PUL/CRV-γCD-IC NF during shelf-life.

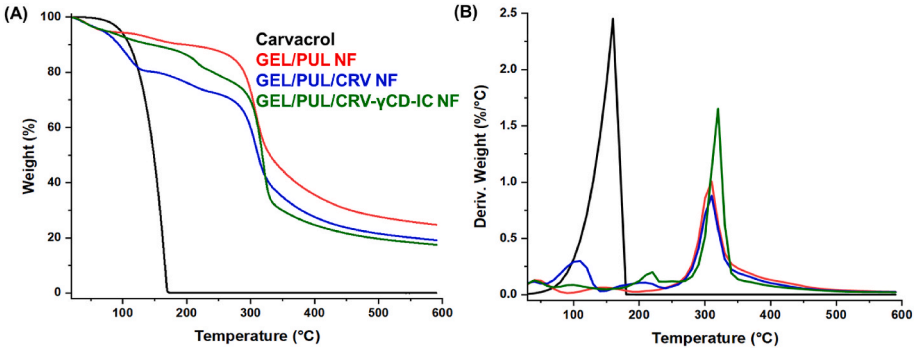

Fig. 4. (A) TGA thermograms and (B) derivatives of γCD powder, GEL/PUL, GEL/PUL/CRV, and GEL/PUL/CRV-γCD-IC NFs.

3.4. Antioxidant activity

Carvacrol is a phenolic monoterpene compound that exhibits antioxidant properties because of chain breaking activity of phenolic components. Carvacrol molecules prevent oxidation by proton donation and cause their own oxidation. After then, their polarity gets stabilized by means of electron dislocation. The antioxidant bioactivity of carvacrol is the outcome of this process (Gursul et al., 2019; Zeb, 2020). Here, the DPPH• assay was performed to assess the antioxidant capacity of samples. In this method, antioxidant molecules reduce the DPPH radical, and the colour of the solution turns from violet to yellowish based on electron transfer (Brand-Williams et al., 1995). The UV–Vis absorption spectra of GEL/PUL NF, GEL/PUL/CRV NF, GEL/PUL/CRV-γCD-IC NF, and DPPH• solution were recorded between the wavelengths of 400–800 nm since the DPPH• shows the maximum absorption at 517 nm (Fig. 6A). The DPPH• solution included GEL/PUL NF was purple, whereas the carvacrol loaded ones exhibited a yellowish colour after 48 h incubation (Fig. 6B). The antioxidant activities of GEL/PUL/CRV NF and GEL/PUL/CRV-γCD-IC NF were tested at sample concentrations ranging from 125 μg/mL to 2000 μg/mL. GEL/PUL NF was also prepared in the determined concentration range and used as a control. The IC50 values were calculated using the radical inhibition (%) data as a function of sample concentration for 30 min period. The IC50 value denotes the quantity of antioxidant material required to reduce the initial concentration of DPPH radicals by 50% (de Menezes et al., 2021). The IC values of GEL/PUL/CRV NF and GEL/PUL/CRV-γCD-IC NF were determined as 701 g/mL and 692 g/mL, respectively and lower value showed the higher antioxidant capacity of GEL/PUL/CRV-γCD-IC NF compared to GEL/PUL/CRV NF.

The time-dependent inhibition graph demonstrated that 97.93% of inhibition was achieved within 48 h by GEL/PUL/CRV-γCD-IC NF (Fig. 6B). On the other hand, GEL/PUL/CRV NF had 93.24% inhibition of DPPH• activity. The DPPH radical was reduced by the strong hydrogen-donating ability of the carvacrol. The control sample of GEL/PUL NF slightly affected inhibition (24.32%). While pure pullulan and γCD do not affect DPPH• inactivation, the radical scavenging capacity of GEL/PUL NFs originates from antioxidant peptide fractions of fish gelatin (Celebioglu & Uyar, 2021; Kwak et al., 2021). GEL/PUL/CRV-γCD-IC NF had significantly higher antioxidant potential than other samples after 48 h ($p < 0.05$). These results showed that inclusion complexation did not obstruct the radical scavenging activity of carvacrol. In a related study, Celebioglu and Uyar (2021) reported that the γCD inclusion complex did not also limit the radical scavenging ability of the eugenol compound since its phenolic group was oriented on the broader rim of CD. The methyl and phenolic hydroxyl groups of carvacrol can be found at either the broad or narrow rim of the CD molecule since the cavity size is wide enough. (Yildiz et al., 2018). The geometrical accommodation of carvacrol in complex structure provided higher encapsulation efficiency. Here, the activity and stability of carvacrol were evolved by inclusion complexation and the results of the antioxidant activity tests confirmed the potential of these nanofibers to be used in food packaging applications.

3.5. Food application and oxidative stability

Fish oil is one of the most widely used food supplements worldwide and contains nutritionally valuable fatty acids. However, its polyunsaturated fatty acids are very susceptible to degradation. The breakdown of polyunsaturated long-chain fatty acids into smaller molecules forms hydroperoxides that tend to decompose into undesired volatile components such as ketones, aldehydes, and carboxylic acids (Lembke & Schubert, 2014). Oxidative degradation is the main problem that reduces the shelf life of fish oil. Therefore, protecting fish oil against oxidation is the primary concern during processing, transportation, and storage. Oxidation may be avoided by restricting the presence of oxygen, establishing an inert atmosphere, and adding synthetic or natural antioxidants to the oil content (Jairoun et al., 2020; Mozuraityte et al., 2016). Liquid fish oil can be kept in an inert atmosphere to avoid oxidation, but this is not practical for consumers once the bottle has been opened. In this study, fish oils were stored at 40 °C and under the atmospheric air without a particular inert environment. As depicted in Fig. 7A, nanofibers were placed on the inner face of the lids and not in contact with fish oil.

The oxidation degree of oils during accelerated storage was quantified by the analyses of peroxide value (PV) and conjugated dienes. The PV results of fish oil samples were summarized in Fig. 7B. The initial PV was found as 6.15 ± 0.07 meq O_2/kg oil. The PV increased for each sample in the first four days and this increase kept up until the 8th day of storage. The control fish oil group, without attached nanofiber in the lid, reached the highest PV which is 42.83 meq O_2/kg oil at 8 days of storage at 40 °C. The PV of GEL/PUL NF, and GEL/PUL/CRV NF were significantly higher compared to GEL/PUL/CRV-γCD-IC NF at the fourth day. ($p < 0.05$). Both GEL/PUL/CRV NF and GEL/PUL/CRV-CD-IC NF displayed considerable variations from the control sample by the eighth day. The samples that significantly vary from the control are pointed out in Fig. 7B. The PV was decreased after 8 days due to the breakdown of hydroperoxides to secondary oxidation products. The statistical analysis indicated that the carvacrol-loaded nanofibers achieved a delay in the oxidation of oil samples and the highest impact was observed by GEL/PUL/CRV-γCD-IC NF during 8-day storage ($p < 0.05$).

The unsaturated fatty acids in fish oil were oxidized during accelerated storage, leading to a change in double bond positions and the formation of conjugated double bonds. Since the formation of conjugated dienes increases UV absorption, it is used to determine the oxidation level of the product (Khor et al., 2021). The changes in conjugated dienes of fish oil samples were represented in Fig. 7C. As

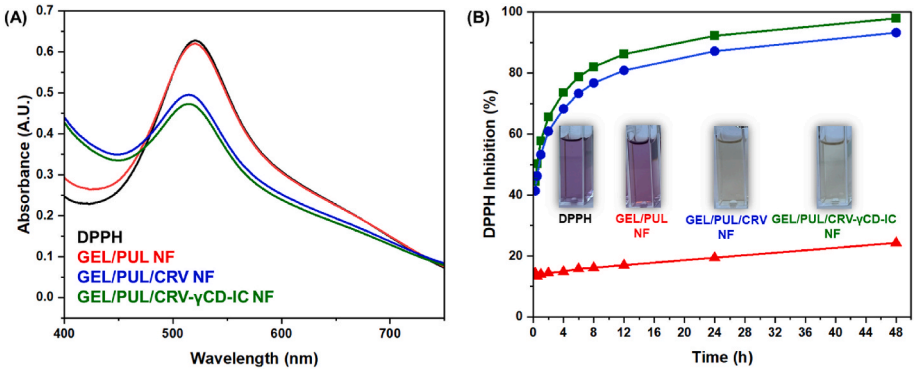

Fig. 6. (A) The UV–Vis absorption spectra of DPPH• solution and GEL/PUL NF, GEL/PUL/CRV NF, GEL/PUL/CRV-γCD-IC NF at the concentration of 0.5 mg NF/mL after 30 min incubation. (B) Time-dependent antioxidant performance graph and the representative solution photos of nanofibers after 48 h incubation.

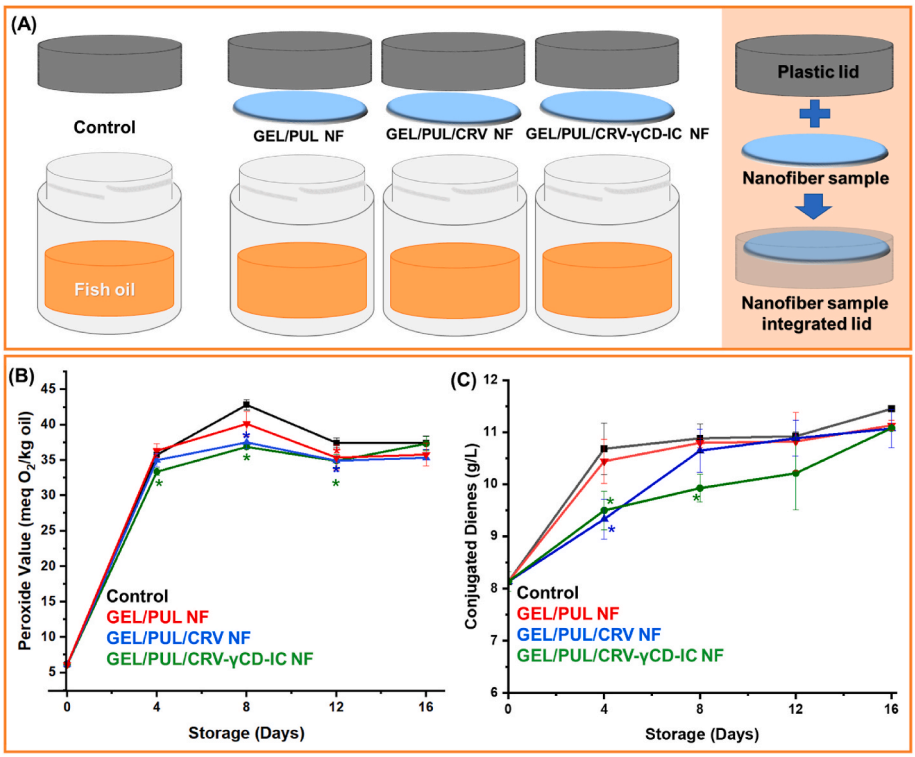

Fig. 7. (A) Food system application of nanofiber samples and control fish oil. (B) Peroxide value and (C) conjugated dienes concentration of fish oil during accelerated storage. Data points having the * symbol significantly differ from the control sample ($p \leq 0.05$).

expected, the conjugated diene values were increased during storage. The conjugated dienes value of control fish oil, which was initially determined as 8.13 g/L, reached 10.68 g/L after four days. High polyunsaturated fatty acid concentrations may contribute to the rapid development of conjugated dienes (Liu & White, 1992). Hence, at the beginning of the storage, a sharp increase was observed in conjugated diene concentrations of each fish oil sample. Nanofiber free control samples had similar behaviour with GEL/PUL NF integrated system, while GEL/PUL/CRV NF and GEL/PUL/CRV-γCD-IC NF significantly decelerated the formation of conjugated dienes up to day eight ($p < 0.05$). Carvacrol activity of GEL/PUL/CRV NF on oxidation rate began to decline in later stages. GEL/PUL/CRV-γCD-IC NF integrated systems were able to reduce conjugated diene formation until day 12, possibly due to efficient encapsulation and controlled release of carvacrol. Although conjugated dienes displayed of increase during the oxidation test, the PVs exhibited an increase and then a decrease. The reason for the different trends is that conjugated dienes outlast hydroperoxides because they remain intact (Schaich et al., 2013). Besides PV results, conjugated dienes values confirmed that GEL/PUL/CRV-γCD-IC NF retarded oxidation at 40 °C and under ambient air.

3.6. Antimicrobial activity

The growth curve assay was performed to assess the antibacterial property of nanofibers, and graphs were given in Fig. 8. Different strains of Gram-positive and Gram-negative bacteria, including *Escherichia coli*, *Salmonella enterica* serovar Typhimurium 14028s and *Staphylococcus aureus,* were cultured to test a broad range of activity. Streptomycin was used as a positive control. Different concentrations of carvacrol (2.5, 5, and 10 mg/mL) were also examined for each microorganism. To assess bacterial viability OD_{600} was recorded every 30 min for 20 h. The antimicrobial activity of the samples was also evaluated by disk-diffusion assay. Although the results gave an insight into the antimicrobial activity of the nanofibers, they were not reported here since the zones were overlapped and unclear but used as supplementary information (Fig. S3). Streptomycin and carvacrol demonstrated similar activity against microorganisms. As shown in Fig. 8, the GEL/PUL/CRV-γCD-IC NF demonstrated better antibacterial activity against the tested microorganisms as compared to the GEL/PUL/CRV NF ($p < 0.05$). As expected, bacterial viability in GEL/PUL NF treatment were similar to that of sample-free DMSO. The incubation period includes different phases of microorganism growth which are the lag, logarithmic and stationary phases (Adkar et al., 2017). GEL/PUL/CRV NF extended the lag phase for all strains of bacteria. In the beginning, there was a noticeable effect on bacterial growth. After 3 h of incubation, the lowest concentration (25 mg/mL) of GEL/PUL/CRV NF showed increased growth in both Gram-positive and Gram-negative bacteria. The growth-inhibiting effect on the bacteria significantly increased as the nanofiber concentration increased ($p < 0.05$). For example, the inhibition rates of the GEL/PUL/CRV-γCD-IC NF at 25 mg/mL and 50 mg/mL concentrations were calculated as 34.1% and 60.6% relative to DMSO, while the concentration of 100 mg/mL provided complete growth inhibition of Gram-negative *E. coli.* Although the nanofibers brought about different inhibition rates in tested bacterial strains, their antibacterial activities were sorted against Gram-positive *S. aureus* and Gram-negative *S. enterica* as follows: GEL/PUL/CRV-γCD-IC NF > GEL/PUL/CRV NF > GEL/PUL NF.

The highest concentration of the GEL/PUL/CRV-γCD-IC NF acted like the antibiotic streptomycin for Gram-negative microorganisms. The growth of both *E. coli* and *S. enterica* was completely inhibited by GEL/PUL/CRV-γCD-IC NF at the highest concentration of nanofiber, whereas *S. aureus* showed minimal growth after 18-h incubation. Although several studies have hypothesized (Ait-Ouazzou et al., 2012; Amjadi et al., 2022; Wen et al., 2016) that Gram-negative bacteria are more resistant against essential oils than Gram-positives due to divergences in cell wall patterns, various researchers reported contrary results for carvacrol (Kurek et al., 2014; Tampau et al., 2018) and citrus essential oils (Ambrosio et al., 2019). The outer membrane found in Gram-negative bacteria is absent in Gram-positive bacteria. This outer membrane has transmembrane channels (porins) and

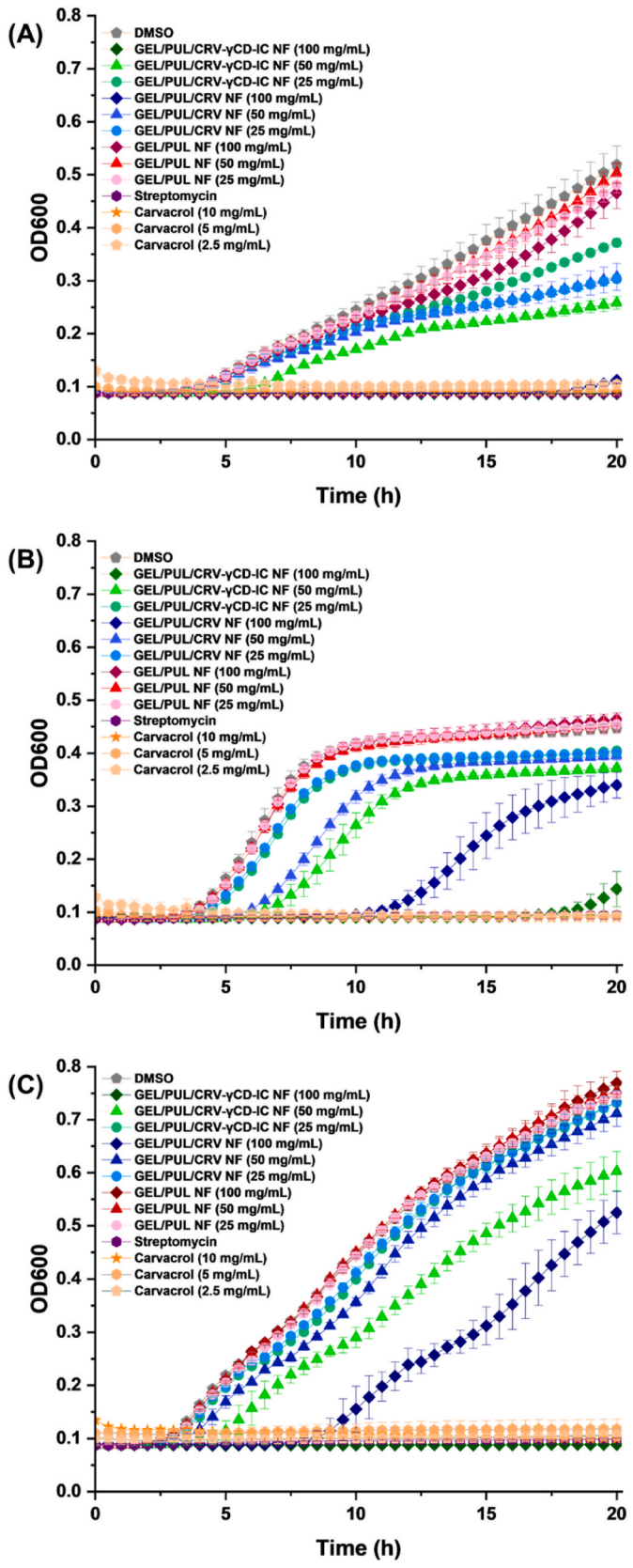

Fig. 8. Growth curves of samples against (A) *E. coli*, (B) *S. aureus*, and (C) *S. enterica*.

lipopolysaccharides with polar ends that allow the passage of hydrophilic compounds while impeding the diffusion of hydrophobic molecules, such as essential oils, into the cytoplasm (Marinelli et al., 2018). In this study, the enhanced hydrophilic character, and the varying polarity of the GEL/PUL/CRV-γCD-IC NF, which is a result of inclusion complexation, may account for the decelerated rate of growth. On the other hand, the similar trend in antibacterial activity of GEL/PUL/CRV NF against Gram-negative and -positive bacteria can be attributed to several proposed mechanisms of carvacrol including leaking of cell contents, cytoplasm coagulation, inhibition of motility, damage of cytoplasmic membrane and membrane protein (Burt, 2004).

4. Conclusion

In this study, the inclusion complexes of carvacrol-γCD were incorporated into electrospun nanofibers of gelatin/pullulan biopolymers (GEL/PUL/CRV-γCD-IC NF). Carvacrol retention, at 10% initial concentration, was found to differ significantly during the electrospinning process and the storage for GEL/PUL/CRV-γCD-IC NF and the control sample of GEL/PUL/CRV NF. The inclusion complexation resulted in higher preservation during storage at room temperature and enhanced the shelf-life. In addition, carvacrol evaporation from the solution during the electrospinning process was substantially prevented. The free-standing and flexible nanofibers were obtained for both GEL/PUL/CRV-γCD-IC and GEL/PUL/CRV systems. While a smooth nanofiber formation was observed for GEL/PUL/CRV NF, the inclusion complex crystals were detected throughout GEL/PUL/CRV-γCD-IC NF. The inclusion complexation ensured thermal stability and delayed the volatilization for carvacrol. Inclusion complexation is also an efficient way to enhance the water solubility of essential oil carvacrol by the lipophilic cavity, provided highly stable encapsulation without hindering the antioxidant and antibacterial activity. The promising antioxidant activity of nanofibers delayed fish oil oxidation, and the GEL/PUL/CRV-γCD-IC NF had the most significant influence. The increased hydrophilic character of carvacrol in GEL/PUL/CRV-γCD-IC NF led to the remarkable inhibitory activity of the active compound against Gram-negative bacteria. As this research has demonstrated, gelatin/pullulan nanofibers loaded inclusion complex of γCD with carvacrol have further potential with the promoted thermal, antimicrobial, and antioxidant characteristics, which are highly desirable properties for active food packaging systems. Because of its bioactivity, this developed electrospun nanofiber can be used to package foods susceptible to oxidation, extend the shelf life of foods by preventing microbial spoilage, and ensure food safety. The packaging material developed from pullulan and gelatin biopolymers offers sustainability and serves green practices.

CRediT authorship contribution statement

Kubra Ertan: Conceptualization, Methodology, Validation, Investigation, Writing-Original draft preparation.

Asli Celebioglu: Conceptualization, Methodology, Validation, Investigation, Review & Editing.

Rimi Chowdhury: Investigation and Methodology of Antibacterial activity studies, Writing–Original draft related to antibacterial activity studies.

Gulum Sumnu: Supervision, Review & Editing.

Serpil Sahin: Supervision, Review & Editing.

Craig Altier: Supervision, Resources, Review & Editing of original draft related to antibacterial activity studies.

Tamer Uyar: Supervision, Resources, Conceptualization, Methodology, Project administration, Funding acquisition, Review & Editing.

Declaration of competing interest

The authors declare that they have no known competing financial interests or personal relationships that could have appeared to influence

the work reported in this paper.

Data availability

Data will be made available on request.

Acknowledgements

This work made use of the Cornell Center for Materials Research Shared Facilities which are supported through the NSF MRSEC program (DMR-1719875), and Department of Human Centered Design facilities. Kubra Ertan gratefully thanks The Scientific and Technological Research Council of Turkey (TUBITAK) for the financial support (TUBITAK-BIDEB 2214A Fellowship program). The authors thank M. Alishahi for re-preparation of carvacrol-γCD-inclusion complex solution and measuring the pH of pullulan/gelatin solution for the revised version.

Appendix A. Supplementary data

Supplementary data to this article can be found online at https://doi.org/10.1016/j.foodhyd.2023.108864.

References

Aceituno-Medina, M., Mendoza, S., Lagaron, J. M., & López-Rubio, A. (2013). Development and characterization of food-grade electrospun fibers from amaranth protein and pullulan blends. *Food Research International, 54*(1), 667–674. https://doi.org/10.1016/j.foodres.2013.07.055

Adkar, B. V., Manhart, M., Bhattacharyya, S., Tian, J., Musharbash, M., & Shakhnovich, E. I. (2017). Optimization of lag phase shapes the evolution of a bacterial enzyme. *Nature Ecology and Evolution, 1*, 1–6. https://doi.org/10.1038/s41559-017-0149

Ait-Ouazzou, A., Espina, L., Gelaw, T. K., de Lamo-Castellví, S., Pagán, R., & García-Gonzalo, D. (2012). New insights in mechanisms of bacterial inactivation by carvacrol. *Journal of Applied Microbiology, 114*, 173–185. https://doi.org/10.1111/jam.12028

Altan, A., Aytac, Z., & Uyar, T. (2018). Carvacrol loaded electrospun fibrous films from zein and poly(lactic acid) for active food packaging. *Food Hydrocolloids, 81*, 48–59. https://doi.org/10.1016/j.foodhyd.2018.02.028

Ambrosio, C. M. S., Ikeda, N. Y., Miano, A. C., Saldaña, E., Moreno, A. M., Stashenko, E., Contreras-Castillo, C. J., & Da Gloria, E. M. (2019). Unraveling the selective antibacterial activity and chemical composition of citrus essential oils. *Scientific Reports, 9*, Article 17719. https://doi.org/10.1038/s41598-019-54084-3

Amjadi, S., Gholizadeh, S., Ebrahimi, A., Almasi, H., Hamishehkar, H., & Taheri, R. A. (2022). Development and characterization of the carvone-loaded zein/pullulan hybrid electrospun nanofibers for food and medical applications. *Industrial Crops and Products, 183*, Article 114964. https://doi.org/10.1016/j.indcrop.2022.114964

Arrieta, M. P., Peltzer, M. A., Garrigós, M., del, C., & Jiménez, A. (2013). Structure and mechanical properties of sodium and calcium caseinate edible active films with carvacrol. *Journal of Food Engineering, 114*, 486–494. https://doi.org/10.1016/j.jfoodeng.2012.09.002

Aytac, Z., Ipek, S., Durgun, E., Tekinay, T., & Uyar, T. (2017). Antibacterial electrospun zein nanofibrous web encapsulating thymol/cyclodextrin-inclusion complex for food packaging. *Food Chemistry, 233*, 117–124. https://doi.org/10.1016/j.foodchem.2017.04.095

Aytac, Z., Keskin, N. O. S., Tekinay, T., & Uyar, T. (2017). Antioxidant α-tocopherol/γ-cyclodextrin–inclusion complex encapsulated poly(lactic acid) electrospun nanofibrous web for food packaging. *Journal of Applied Polymer Science, 134*, Article 44858. https://doi.org/10.1002/app.44858

Bayir, A. G., Kiziltan, H. S., & Kocyigit, A. (2019). Plant family , carvacrol , and putative protection in gastric cancer. In R. R. Watson, & V. R. Preedy (Eds.), *Dietary interventions in gastrointestinal diseases* (pp. 3–18). Academic Press. https://doi.org/10.1016/B978-0-12-814468-8.00001-6.

Brand-Williams, W., Cuvelier, M. E., & Berset, C. (1995). Use of a free radical method to evaluate antioxidant activity. *LWT - Food Science and Technology, 28*(1), 25–30. https://doi.org/10.1016/S0023-6438(95)80008-5

Burt, S. (2004). Essential oils: Their antibacterial properties and potential applications in foods—a review. *International Journal of Food Microbiology, 94*(3), 223–253. https://doi.org/10.1016/j.ijfoodmicro.2004.03.022

Celebioglu, A., Ipek, S., Durgun, E., & Uyar, T. (2017). Selective and efficient removal of volatile organic compounds by channel-type gamma-cyclodextrin assembly through inclusion complexation. *Industrial & Engineering Chemistry Research, 56*(25), 7345–7354. https://doi.org/10.1021/acs.iecr.7b01084

Celebioglu, A., & Uyar, T. (2021). Electrohydrodynamic encapsulation of eugenol-cyclodextrin complexes in pullulan nanofibers. *Food Hydrocolloids, 111*, Article 106264. https://doi.org/10.1016/j.foodhyd.2020.106264

Cid-Samamed, A., Rakmai, J., Mejuto, J. C., Simal-Gandara, J., & Astray, G. (2022). Cyclodextrins inclusion complex: Preparation methods, analytical techniques and food industry applications. *Food Chemistry, 384*, Article 132467. https://doi.org/10.1016/j.foodchem.2022.132467

Crini, G., Fourmentin, S., Fenyvesi, É., Torri, G., Fourmentin, M., & Morin-Crini, N. (2018). Cyclodextrins, from molecules to applications. *Environmental Chemistry Letters, 16*, 1361–1375. https://doi.org/10.1007/s10311-018-0763-2

Dai, Q., Huang, X., Jia, R., Fang, Y., & Qin, Z. (2022). Development of antibacterial film based on alginate fiber, and peanut red skin extract for food packaging. *Journal of Food Engineering, 330*, Article 111106. https://doi.org/10.1016/j.jfoodeng.2022.111106

Dierings de Souza, E. J., Kringel, D. H., Dias, A. R. G., & da Rosa Zavareze, E. (2021). Polysaccharides as wall material for the encapsulation of essential oils by electrospun technique. *Carbohydrate Polymers, 265*, Article 118068. https://doi.org/10.1016/j.carbpol.2021.118068

Drosou, C., Krokida, M., & Biliaderis, C. G. (2018). Composite pullulan-whey protein nanofibers made by electrospinning: Impact of process parameters on fiber morphology and physical properties. *Food Hydrocolloids, 77*, 726–735. https://doi.org/10.1016/j.foodhyd.2017.11.014

Duconseille, A., Astruc, T., Quintana, N., Meersman, F., & Sante-Lhoutellier, V. (2015). Gelatin structure and composition linked to hard capsule dissolution: A review. *Food Hydrocolloids, 43*, 360–376. https://doi.org/10.1016/j.foodhyd.2014.06.006

Ferreira, A. R. V., Bandarra, N. M., Moldão-Martins, M., Coelhoso, I. M., & Alves, V. D. (2018). FucoPol and chitosan bilayer films for walnut kernels and oil preservation. *LWT - Food Science and Technology, 91*, 34–39. https://doi.org/10.1016/j.lwt.2018.01.020

Fonseca, L. M., Cruxen, C. E., dos, S., Bruni, G. P., Fiorentini, Â. M., Zavareze, E. da R., Lim, L. T., & Dias, A. R. G. (2019). Development of antimicrobial and antioxidant electrospun soluble potato starch nanofibers loaded with carvacrol. *International Journal of Biological Macromolecules, 139*, 1182–1190. https://doi.org/10.1016/j.ijbiomac.2019.08.096

Friedman, M. (2014). Chemistry and multibeneficial bioactivities of carvacrol (4-isopropyl- 2-methylphenol), a component of essential oils produced by aromatic plants and spices. *Journal of Agricultural and Food Chemistry, 62*, 7652–7670.

Ghorani, B., Emadzadeh, B., Rezaeinia, H., & Russell, S. J. (2020). Improvements in gelatin cold water solubility after electrospinning and associated physicochemical , functional and rheological properties. *Food Hydrocolloids, 104*, Article 105740. https://doi.org/10.1016/j.foodhyd.2020.105740

Gounga, M. E., Xu, S. Y., & Wang, Z. (2007). Whey protein isolate-based edible films as affected by protein concentration, glycerol ratio and pullulan addition in film formation. *Journal of Food Engineering, 83*(4), 521–530. https://doi.org/10.1016/j.jfoodeng.2007.04.008

Guo, M., Wang, H., Wang, Q., Chen, M., Li, L., Li, X., & Jiang, S. (2020). Intelligent double-layer fiber mats with high colorimetric response sensitivity for food freshness monitoring and preservation. *Food Hydrocolloids, 101*, Article 105468. https://doi.org/10.1016/j.foodhyd.2019.105468

Gursul, S., Karabulut, I., & Durmaz, G. (2019). Antioxidant efficacy of thymol and carvacrol in microencapsulated walnut oil triacylglycerols. *Food Chemistry, 278*, 805–810. https://doi.org/10.1016/j.foodchem.2018.11.134

Hadian, Z., Kamalabadi, M., Phimolsiripol, Y., Balasubramanian, B., Lorenzo Rodriguez, J. M., & Mousavi Khaneghah, A. (2023). Preparation, characterization, and antioxidant activity of β-cyclodextrin nanoparticles loaded Rosa damascena essential oil for application in beverage. *Food Chemistry, 403*, Article 134410. https://doi.org/10.1016/j.foodchem.2022.134410

Hattrem, M. N., Molnes, S., Haug, I. J., & Draget, K. I. (2015). Interfacial and rheological properties of gelatin based solid emulsions prepared with acid or alkali pretreated gelatins. *Food Hydrocolloids, 43*, 700–707. https://doi.org/10.1016/j.foodhyd.2014.07.026

Islam, M. S., & Yeum, J. H. (2013). Electrospun pullulan/poly(vinyl alcohol)/silver hybrid nanofibers: Preparation and property characterization for antibacterial activity. *Colloids and Surfaces A: Physicochemical and Engineering Aspects, 436*, 279–286. https://doi.org/10.1016/j.colsurfa.2013.07.001

Jairoun, A. A., Shahwan, M., & Zyoud, S. H. (2020). Fish oil supplements, oxidative status, and compliance behaviour: Regulatory challenges and opportunities. *PLoS One, 15*(12), Article e0244688. https://doi.org/10.1371/journal.pone.0244688

Kapoor, M. P., Moriwaki, M., Ozeki, M., & Timm, D. (2021). Structural elucidation of novel isoquercitrin-γ-cyclodextrin (IQC-γCD) molecular inclusion complexes of potential health benefits. *Carbohydrate Polymer Technologies and Applications, 2*, Article 100046. https://doi.org/10.1016/j.carpta.2021.100046

Karim, A. A., & Bhat, R. (2008). Gelatin alternatives for the food industry: Recent developments, challenges and prospects. *Trends in Food Science and Technology, 19*, 644–656. https://doi.org/10.1016/j.tifs.2008.08.001

Kayaci, F., Ertas, Y., & Uyar, T. (2013). Enhanced thermal stability of eugenol by cyclodextrin inclusion complex encapsulated in electrospun polymeric nanofibers. *Journal of Agricultural and Food Chemistry, 61*(34), 8156–8165. https://doi.org/10.1021/jf402923c

Kayaci, F., & Uyar, T. (2012). Encapsulation of vanillin/cyclodextrin inclusion complex in electrospun polyvinyl alcohol (PVA) nanowebs : Prolonged shelf-life and high temperature stability of vanillin. *Food Chemistry, 133*(3), 641–649. https://doi.org/10.1016/j.foodchem.2012.01.040

Khor, Y. P., Wan, S. Y., Tan, C. P., Zhao, G., Li, C., Wang, Y., & Li, Y. (2021). Potential of using basa catfish oil as a promising alternative deep-frying medium : A thermo-oxidative stability study. *Food Research International, 141*, Article 109897. https://doi.org/10.1016/j.foodres.2020.109897

Kraśniewska, K., Pobiega, K., & Gniewosz, M. (2019). Pullulan-biopolymer with potential for use as food packaging. *International Journal of Food Engineering, 15*(9), Article 20190030. https://doi.org/10.1515/ijfe-2019-0030

Kurek, M., Guinault, A., Voilley, A., Galić, K., & Debeaufort, F. (2014). Effect of relative humidity on carvacrol release and permeation properties of chitosan based films and coatings. *Food Chemistry, 144*, 9–17. https://doi.org/10.1016/j.foodchem.2012.11.132

Kutzli, I., Gibis, M., Baier, S. K., & Weiss, J. (2019). Electrospinning of whey and soy protein mixed with maltodextrin – influence of protein type and ratio on the production and morphology of fibers. *Food Hydrocolloids, 93*, 206–214. https://doi.org/10.1016/j.foodhyd.2019.02.028

Kwak, H. W., Park, J., Yun, H., Jeon, K., & Kang, D. (2021). Effect of crosslinkable sugar molecules on the physico-chemical and antioxidant properties of fish gelatin nanofibers. *Food Hydrocolloids, 111*, Article 106259. https://doi.org/10.1016/j.foodhyd.2020.106259

Lembke, P., & Schubert, A. (2014). Introduction to fish oil oxidation, oxidation prevention, and oxidation correction. In R. R. Watson, & F. De Meester (Eds.), *Omega-3 fatty acids in brain and neurological health* (pp. 455–460). Academic Press. https://doi.org/10.1016/b978-0-12-410527-0.00037-5.

Lin, L., Liao, X., Surendhiran, D., & Cui, H. (2018). Preparation of ε-polylysine/chitosan nanofibers for food packaging against Salmonella on chicken. *Food Packaging and Shelf Life, 17*, 134–141. https://doi.org/10.1016/j.fpsl.2018.06.013

Liu, T., Feng, C., Li, Z., Gu, Z., Ban, X., Hong, Y., Cheng, L., & Caiming, L. (2021). Efficient formation of carvacrol inclusion complexes during β-cyclodextrin glycosyltransferase-catalyzed cyclodextrin synthesis. *Food Control, 130*, Article 108296. https://doi.org/10.1016/j.foodcont.2021.108296

Liu, Y., Sameen, D. E., Ahmed, S., Wang, Y., Lu, R., Dai, J., Li, S., & Qin, W. (2022). Recent advances in cyclodextrin-based films for food packaging. *Food Chemistry, 370*, Article 131026. https://doi.org/10.1016/j.foodchem.2021.131026

Liu, H.-R., & White, P. J. (1992). Oxidative stability of soybean oils with altered fatty acid compositions. *Journal of the American Oil Chemists' Society, 69*(6), 528–532. https://doi.org/10.1007/BF02636103

Marinelli, L., Di Stefano, A., & Cacciatore, I. (2018). Carvacrol and its derivatives as antibacterial agents. *Phytochemistry Reviews, 17*, 903–921. https://doi.org/10.1007/s11101-018-9569-x

Mendes, A. C., Stephansen, K., & Chronakis, I. S. (2017). Electrospinning of food proteins and polysaccharides. *Food Hydrocolloids, 68*, 53–68. https://doi.org/10.1016/j.foodhyd.2016.10.022

de Menezes, B. B., Frescura, L. M., Duarte, R., Villetti, M. A., & Barcellos da Rosa, M. (2021). A critical examination of the DPPH method : Mistakes and inconsistencies in stoichiometry and IC50 determination by UV-Vis spectroscopy. *Analytica Chimica Acta, 1157*, Article 338398. https://doi.org/10.1016/j.aca.2021.338398

Menezes, P. P., Serafini, M. R., Santana, B. V., Nunes, R. S., Quintans, L. J., Silva, G. F., Medeiros, I. A., Marchioro, M., Fraga, B. P., Santos, M. R. V., & Araújo, A. A. S. (2012). Solid-state β-cyclodextrin complexes containing geraniol. *Thermochimica Acta, 548*, 45–50. https://doi.org/10.1016/j.tca.2012.08.023

Miyashita, K., Uemura, M., & Hosokawa, M. (2018). Effective prevention of oxidative deterioration of fish oil: Focus on flavor deterioration. *Annual Review of Food Science and Technology, 9*, 209–226. https://doi.org/10.1146/annurev-food-030117-012320

Mosayebi, V., Fathi, M., Shahedi, M., Soltanizadeh, N., & Emam-Djomeh, Z. (2022). Fast-dissolving antioxidant nanofibers based on Spirulina protein concentrate and gelatin developed using needleless electrospinning. *Food Bioscience, 47*, Article 101759. https://doi.org/10.1016/j.fbio.2022.101759

Mozuraityte, R., Kristinova, V., Standal, I. B., Carvajal, A. K., & Aursand, M. (2016). Oxidative stability and shelf life of fish oil. In M. Hu, & C. Jacobsen (Eds.), *Oxidative stability and shelf life of foods containing oils and fats* (pp. 209–231). AOCS Press. https://doi.org/10.1016/B978-1-63067-056-6.00005-7.

Mura, P. (2015). Analytical techniques for characterization of cyclodextrin complexes in the solid state: A review. *Journal of Pharmaceutical and Biomedical Analysis, 113*, 226–238. https://doi.org/10.1016/j.jpba.2015.01.058

Narayanan, G., Boy, R., Gupta, B. S., & Tonelli, A. E. (2017). Analytical techniques for characterizing cyclodextrins and their inclusion complexes with large and small molecular weight guest molecules. *Polymer Testing, 62*, 402–439. https://doi.org/10.1016/j.polymertesting.2017.07.023

Nurilmala, M., Suryamarevita, H., Husein Hizbullah, H., Jacoeb, A. M., & Ochiai, Y. (2022). Fish skin as a biomaterial for halal collagen and gelatin. *Saudi Journal of Biological Sciences, 29*, 1100–1110. https://doi.org/10.1016/j.sjbs.2021.09.056

Schaich, K. M., Shahidi, F., Zhong, Y., & Eskin, N. A. M. (2013). Chapter 11 – lipid oxidation. In N. A. M. Eskin, & F. Shahidi (Eds.), *Biochemistry of foods* (3rd ed., pp. 419–478). Academic Press. https://doi.org/10.1016/B978-0-08-091809-9.00011-X.

Seethu, B. G., Pushpadass, H. A., Emerald, F. M. E., Nath, B. S., Naik, N. L., & Subramanian, K. S. (2020). Electrohydrodynamic encapsulation of resveratrol using food-grade nanofibres : Process optimization, characterization and fortification. *Food and Bioprocess Technology, 13*, 341–354.

Shao, P., Niu, B., Chen, H., & Sun, P. (2018). Fabrication and characterization of tea polyphenols loaded pullulan-CMC electrospun nanofiber for fruit preservation. *International Journal of Biological Macromolecules, 107*, 1908–1914. https://doi.org/10.1016/j.ijbiomac.2017.10.054

Shen, C., Deng, Z., Rao, J., Yang, Z., Li, Y., Wu, D., & Chen, K. (2022). Characterization of glycosylated gelatin/pullulan nanofibers fabricated by multi-fluid mixing solution blow spinning. *International Journal of Biological Macromolecules, 214*(May), 512–521. https://doi.org/10.1016/j.ijbiomac.2022.06.082

Si, Y., Shi, S., & Hu, J. (2023). Applications of electrospinning in human health: From detection, protection, regulation to reconstruction. *Nano Today, 48*, Article 101723. https://doi.org/10.1016/j.nantod.2022.101723

Soto, K. M., Hernández-Iturriaga, M., Loarca-Piña, G., Luna-Bárcenas, G., & Mendoza, S. (2019). Antimicrobial effect of nisin electrospun amaranth : Pullulan nanofibers in apple juice and fresh cheese. *International Journal of Food Microbiology, 295*, 25–32. https://doi.org/10.1016/j.ijfoodmicro.2019.02.001

Sullivan, S. T., Tang, C., Kennedy, A., Talwar, S., & Khan, S. A. (2014). Electrospinning and heat treatment of whey protein nanofibers. *Food Hydrocolloids, 35*, 36–50. https://doi.org/10.1016/j.foodhyd.2013.07.023

Tampau, A., González-Martínez, C., & Chiralt, A. (2018). Release kinetics and antimicrobial properties of carvacrol encapsulated in electrospun poly-(ε-caprolactone) nanofibres. Application in starch multilayer films. *Food Hydrocolloids, 79*, 158–169. https://doi.org/10.1016/j.foodhyd.2017.12.021

Tang, Y., Zhou, Y., Lan, X., Huang, D., Luo, T., Ji, J., Mafang, Z., Miao, X., Wang, H., & Wang, W. (2019). Electrospun gelatin nanofibers encapsulated with peppermint and chamomile essential oils as potential edible packaging. *Journal of Agricultural and Food Chemistry, 67*(8), 2227–2234. https://doi.org/10.1021/acs.jafc.8b06226

Tao, F., Hill, L. E., Peng, Y., & Gomes, C. L. (2014). Synthesis and characterization of β-cyclodextrin inclusion complexes of thymol and thyme oil for antimicrobial delivery applications. *LWT - Food Science and Technology, 59*(1), 247–255. https://doi.org/10.1016/j.lwt.2014.05.037

Topuz, F., & Uyar, T. (2020). Antioxidant, antibacterial and antifungal electrospun nanofibers for food packaging applications. *Food Research International, 130*, Article 108927. https://doi.org/10.1016/j.foodres.2019.108927

Trinetta, V., & Cutter, C. N. (2016). Pullulan : A suitable biopolymer for antimicrobial food packaging applications. In J. Barros-Velázquez (Ed.), *Antimicrobial food packaging* (pp. 385–397). Academic Press. https://doi.org/10.1016/B978-0-12-800723-5.00030-9.

Valderrama, A. C. S., & Rojas De, G. C. (2017). Traceability of active compounds of essential oils in antimicrobial food packaging using a chemometric method by ATR-FTIR. *American Journal of Analytical Chemistry, 8*, 726–741. https://doi.org/10.4236/ajac.2017.811053

Valle, E. M., & Del, M. (2004). Cyclodextrins and their uses : A review. *Process Biochemistry, 39*, 1033–1046. https://doi.org/10.1016/S0032-9592(03)00258-9

Wang, Y., Guo, Z., Qian, Y., Zhang, Z., Lyu, L., & Wang, Y. (2019). Study on the electrospinning of gelatin/pullulan composite nanofibers. *Polymers, 1–10*.

Wang, H., Liu, F., Yang, L., Zu, Y., Wang, H., Qu, S., & Zhang, Y. (2011). Oxidative stability of fish oil supplemented with carnosic acid compared with synthetic antioxidants during long-term storage. *Food Chemistry, 128*, 93–99. https://doi.org/10.1016/j.foodchem.2011.02.082

Wang, Y., Qian, Y., Zhang, Z., Lyu, L., & Wang, Y. (2021). Role of ethanol on crosslinking and properties of electrospun gelatin/pullulan nanofibrous membranes. In *Journal of the textile institute*. https://doi.org/10.1080/00405000.2021.1979336

Weiss, J., Kanjanapongkul, K., Wongsasulak, S., & Yoovidhya, T. (2012). Electrospun fibers: Fabrication, functionalities and potential food industry applications. In Q. Huang (Ed.), *Nanotechnology in the food, beverage and nutraceutical industries* (pp. 362–397). Woodhead Publishing. https://doi.org/10.1533/9780857095657.2.362.

Wen, P., Wen, Y., Zong, M. H., Linhardt, R. J., & Wu, H. (2017). Encapsulation of bioactive compound in electrospun fibers and its potential application. *Journal of Agricultural and Food Chemistry, 65*(42), 9161–9179. https://doi.org/10.1021/acs.jafc.7b02956

Wen, P., Zhu, D. H., Wu, H., Zong, M. H., Jing, Y. R., & Han, S. Y. (2016). Encapsulation of cinnamon essential oil in electrospun nanofibrous film for active food packaging. *Food Control, 59*, 366–376. https://doi.org/10.1016/j.foodcont.2015.06.005

Wong, C. H., Tan, M. Y., Li, X., & Li, D. (2022). Fabrication of electrospun nanofibers with moisture-triggered carvacrol release in fresh produce packaging. *Journal of Food Science, 87*(7), 3129–3137. https://doi.org/10.1111/1750-3841.16206

Yildiz, Z. I., Celebioglu, A., Kilic, M. E., Durgun, E., & Uyar, T. (2018). Fast-dissolving carvacrol/cyclodextrin inclusion complex electrospun fibers with enhanced thermal stability, water solubility, and antioxidant activity. *Journal of Materials Science, 53*, 15837–15849. https://doi.org/10.1007/s10853-018-2750-1

Yilmaz, M. T., Hassanein, W. S., Alkabaa, A. S., & Ceylan, Z. (2022). Electrospun eugenol-loaded gelatin nanofibers as bioactive packaging materials to preserve quality characteristics of beef. *Food Packaging and Shelf Life, 34*, Article 100968. https://doi.org/10.1016/j.fpsl.2022.100968

Zaitoon, A., Lim, L. T., & Scott-Dupree, C. (2021). Activated release of ethyl formate vapor from its precursor encapsulated in ethyl cellulose/poly(ethylene oxide) electrospun nonwovens intended for active packaging of fresh produce. *Food Hydrocolloids, 112*, Article 106313. https://doi.org/10.1016/j.foodhyd.2020.106313

Zeb, A. (2020). Concept, mechanism, and applications of phenolic antioxidants in foods. *Journal of Food Biochemistry, 44*(9), Article e13394. https://doi.org/10.1111/jfbc.13394

Zhan, F., Yan, X., Sheng, F., & Li, B. (2020). Facile in situ synthesis of silver nanoparticles on tannic acid/zein electrospun membranes and their antibacterial, catalytic and antioxidant activities. *Food Chemistry, 330*, Article 127172. https://doi.org/10.1016/j.foodchem.2020.127172